

ATMOSPHERIC SOLAR ABSORPTION MEASUREMENTS IN
THE 9-11 MICRON REGION USING A DIODE
LASER HETERODYNE SPECTROMETER

Charles N. Harward
Department of Physics
Old Dominion University

Norfolk, VA 23508

and

James M. Hoell, Jr.

Langley Research Center

Hampton, VA 23665

ABSTRACT

A tunable diode laser heterodyne radiometer has been developed for ground-based measurements of atmospheric solar absorption spectra in the 9 to 12 micron spectral range. The performance and operating characteristics of this Tunable Infrared Heterodyne Radiometer (TIHR) will be discussed along with recently measured heterodyne solar absorption spectra in the 10-11 micron spectral region.

INTRODUCTION

Fixed frequency or discretely tunable CO₂ laser local oscillators (LO) have been used in heterodyne radiometers to measure selected species of atmospheric or astronomical interest (1), (2), (3), (4), (5), (6). The range of applications have in general depended upon coincidences between CO₂ laser emission wavelengths and absorption lines of the desired species. Often no overlap exists or the close coincidences that are available are contaminated by interferences from other atmospheric species. Far more important, however, for monitoring a wide range of species, is the limited overall coverage available from conventional CO₂ laser systems (i.e., from ~ 9 to 11.5 micrometers). Clearly, the use of passive IR heterodyne techniques would be greatly enhanced through the use of tunable laser LO's operating over a wider spectral region.

Tunable Diode Lasers (TDL) are currently the only commercially available devices that offer the potential for spectral coverage from 3-30 micrometers. These lasers have been successfully used as LO's in heterodyne systems for astronomical observations (7) of the thermal emission from Mars and the moon and for limited stratospheric measurements of solar absorption by ozone (8). Ku and Spears (9) have reported on the use of TDL LO to detect C_2H_4 in a laboratory environment using a 900K blackbody as the source and they also report on excess RF noise generated in a heterodyne system by a diode laser. Additional laboratory studies on the effects of TDL generated noise on heterodyne applications have been reported by (10), (11), (12), and (13). Of particular significance are the results reported by Allario et al (12) demonstrating that the performance of a TDL radiometer can be comparable to that available from a CO_2 laser system.

In this paper, we report on the design and use of a TDL heterodyne radiometer for high resolution ground based atmospheric solar absorption measurements. The performance and operating characteristics of the system will be discussed along with atmospheric absorption of HNO_3 , O_3 , CO_2 , and H_2O in the 9-11 micrometer spectral region. These data along with additional spectra to be obtained with this system, when coupled to existing Fourier transform spectra (14) will be useful for identifying optimum LO wavelengths for future tropospheric and stratospheric monitoring.

EXPERIMENTAL DETAILS

The Tunable Infrared Heterodyne Radiometer (TIHR) discussed here is shown in figure 1. It is currently coupled to an eight inch heliostat located on the roof of a laboratory at Langley Research Center, Hampton, VA. The current version of the TIHR is designed to operate over the spectral region from 8 to 12 microns. The lower wavelength cutoff is dictated by a long pass optical filter in the solar path, while the long wavelength cutoff is due to the spectral response of the high speed HgCdTe photomixer. The TDL's are mounted in a commercially available closed cycle cooler modified to reduce frequency fluctuations in the laser output. Radiation from the TDL is collected and collimated by an f/1 Ge lens. The monochromator shown in figure 1 is only used for coarse wavelength characterization and identification. During operation of the radiometer, the monochromator is bypassed by using the first flip mirror and for multimode laser operation, a scanning etalon is inserted in the optical path to isolate and track a single TDL mode. The TDL and solar radiation are combined at the 1:1 ZnSe beamsplitter and then focused onto a LN_2 cooled HgCdTe photomixer with an f/2 Ge lens. The incoming solar radiation from the heliostat (or 1300K blackbody for calibration and alignment) is mechanically chopped and filtered using the eight micron long pass optical filter. The TDL radiation reflected by the beamsplitter is directed into a wavelength identification system similar to that used in standard TDL spectroscopic systems. The gas cell, with a suitable reference gas, provides an absolute frequency scale while the solid Ge etalon provides a relative frequency scale to account for the nonlinear tuning rate of the laser over

extended wavelength regions and between absorption lines from the reference gas.

One of the advantages of tunable LO's is that the radiometer can be used either as a scanning or fixed frequency system. As a fixed frequency system, the TIHR utilizes a wide bandwidth photomixer and IF amplifier (i.e., 5-2000 MHz). The IF output is channelized using up to 16 IF filters. The output from each filter is rectified by a crystal detector and synchronously detected by a lock-in amplifier referenced to the chopper in the solar path. In the scanning mode reported here, the wideband width amplifier is replaced with a lower noise amplifier, having a much narrower bandwidth (i.e., 1-200 MHz), a single 100 MHz bandwidth low pass IF filter, crystal detector and lock-in amplifier. The scanning mode offers the advantage of wider spectral coverage limited only by the tuning range of the TDL. The fixed frequency operation, however, offers a multiplex advantage through the use of multiple IF channels which can be important for quantitative measurements of trace molecules.

It is well known that the gain curve of lead salt lasers is broad enough to sustain several longitudinal modes in its emission spectrum. For most applications, a single longitudinal mode is desired. To facilitate the use of the scanning mode of the TIHR, the etalon shown in figure 1 was used to isolate and track a single longitudinal mode. Use of an etalon for mode isolation provides a simple compact technique with high throughput. Furthermore, the center of the bandpass curve for the etalon can easily be locked to the peak of an individual mode for operation over an extended spectral range. The electronic feedback system used for tracking the TDL was assembled using standard components. After centering the etalon transmission peak on the desired TDL mode, a small 1000 Hz AC dither voltage obtained from the internal oscillator of a lock-in amplifier was applied to the etalon control voltage. Near the etalon transmission peak the TDL radiation is modulated such that the modulation amplitude is proportional to the offset between the peak of the etalon transmission curve and the isolated TDL mode; the phase of the modulated TDL signal relative to the dither voltage depends on which side of the etalon transmission curve the isolated mode is located. Therefore, a phase/amplitude dependent signal is obtained by synchronously detecting the modulation on the DC current generated in the photomixer by the TDL radiation. This is used to control the etalon plate spacing via a variable gain high voltage amplifier internal to the etalon control module. To minimize the effects on the heterodyne signal, the dither frequency was chosen to be an odd multiple of the chopper frequency in the solar path and much larger than the effective post integration frequency. Figures 2a and 2b illustrate the operation of the tracking etalon. The upper trace in each figure is the heterodyne signal obtained using a 1300K blackbody source while the lower trace is the output of the solid etalon in the wavelength identification section. In figure 2a, the general shape of the heterodyne signal results from the convolution of the TDL power curve and the bandpass function of the static etalon. In figure 2b, where the etalon is locked to the peak of the TDL mode, there is little variation in the TDL power curve over the same tuning range used in figure 2a. More important, the continuous spectral coverage is now limited only by the tuning range of the individual mode and the overall signal variation is now due to the true variation in laser power.

ATMOSPHERIC SOLAR ABSORPTION

Table I gives the spectral regions that have been covered to date using two lead salt lasers; one provided by Dr. Wayne Lo, from General Motors Research Laboratory, and the other obtained from Laser Analytics, Inc. Figures 3, 4, and 5 show spectra in which all the features have been identified. For the data shown here, the LO power ranged from about 200 to 300 microwatts. Each spectra was recorded in the scanning mode with a 100 MHz low pass IF filter (i.e., spectral resolution $\sim .007 \text{ cm}^{-1}$) and a post integration time of 2.5 secs. The measured signal-to-noise ratio (SNR) ranged from 200 to 300. For the above system parameters, the maximum expected SNR viewing the unattenuated solar energy is approximately 800. Atmospheric attenuation, mismatch between the TDL and signal wavefronts along with uncertainties in some system parameters such as optical throughput and photomixer efficiency explain the lower SNR actually measured. The data shown in figure 3 includes the atmospheric solar absorption spectra from 921.1 cm^{-1} to 921.6 cm^{-1} ; the absolute frequency mark was obtained from the wavelength ID gas cell with ammonia as the calibration gas, and the relative frequency marks from the solid germanium etalon. The only feature seen in the atmospheric spectra is attributed to water vapor. It is interesting to note that for this spectral region atmospheric ammonia should be discernible at tropospheric levels greater than 1 ppb. Also, note that the halfwidth of the water vapor absorption is approximately 3 GHz as expected for a tropospheric species. Figure 4 shows a spectral region exhibiting ozone absorption features with halfwidths which can be attributed to stratospheric pressure broadening and a CO_2 feature with a halfwidth consistent with tropospheric broadening. The absolute wavelength for this spectra was obtained from the R(34) ($0001 - 0200$) CO_2 feature. This spectrum also shows the affect of a longitudinal mode change in the TDL emission which occurs at the point separation regions 1 and 2 where region 1 is near 1086.8 cm^{-1} and region 2 is near 1088.6 cm^{-1} . Figure 5 shows the atmospheric absorption spectra from about 896.0 cm^{-1} to 896.6 cm^{-1} , along with two reference spectra from the wavelength identification section of the TIHR. The reference spectra is for pure HNO_3 (upper trace) and low pressure HNO_3 broadened by approximately 50 torr of air (middle trace). The fine structure seen in the atmospheric spectra can be attributed to stratospheric nitric acid. The wavelengths identified on this figure were obtained from Brockman et al. (15). The broad feature at 896.507 cm^{-1} has been attributed to absorption primarily by H_2O and CO_2 . It is significant to note that lower resolution ($.02 \text{ cm}^{-1}$) ground based data (14) available for this region shows only the H_2O and CO_2 absorption and little if any of the HNO_3 fine structure seen in figure 5. Figure 6 shows a synthetic atmospheric spectra generated using the line parameters for CO_2 , H_2O , (16) and HNO_3 (15). With the exception of the overall shape of the experimental data due to the TDL power variation, the similarity between the synthetic spectrum and the experimental spectrum is evident. With the addition of a blackbody calibration source, the experimental data could be used to obtain HNO_3 profiles.

SUMMARY

In summary, we have shown the design and operating characteristics of a tunable infrared heterodyne radiometer which uses a tunable diode laser as a local oscillator. The use of a scanning etalon as a mode isolator as well as the improvement in system performance when the etalon was locked to the TDL was shown. Atmospheric absorption spectra of selected regions from the 9 and 11 micrometer were presented. These data exhibited the highest resolution HNO_3 atmospheric spectra obtained to date and demonstrated the ability of the TIHR to discriminate between absorption which occurs in different atmospheric regions.

REFERENCES

1. Abbas, Mian M.; Kosluk, Theodore; Mumma, Michael J.; Buhl, David; Kunde, Virgil G.; and Brown, Larry W.: Stratospheric Ozone Measurement with an Infrared Heterodyne Spectrometer. *Geophy. Res. Lett.*, 5, 317-320, 1978.
2. Betz, A. L.; Johnson, M. A.; McLaren, R. A.; and Sutton, E. C.: Heterodyne Detection of CO₂ Emission Lines and Wind Velocities in the Atmosphere of Venus, *Astrophys. J.*, 208, L141, 1976.
3. Hoell, J.; Harward, C.; and Williams, B.: Remote Infrared Heterodyne Radiometer Measurements of Atmospheric Ammonia Profiles. *Geophy. Res. Lett.*, 7, 1980.
4. Menzies, Robert T.: Atmospheric Monitoring Using Heterodyne Detection Techniques. *Optical Eng.*, 17, 44-49, Jan. - Feb. 1978.
5. Mumma, Michael J.; Kostouk, Theodor; Buhl, David: A 10 μ m Laser Heterodyne Spectrometer for Remote Detection of Trace Gases. *Optical Eng.*, 17, 50-55, Jan. - Feb. 1978.
6. Peyton, B. J.; Lange, R. A.; Savage, M. G.; Seals, R. K.; and Allario, F.: AIAA Paper 77-73, AIAA 15th Aerospace Sciences Meeting, Los Angeles, CA, Jan. 24-26, 1977.
7. Mumma, M.; Kostiuik, I.; Cohen, S.; Buhl, D.; and von Thuna, P. C.: Infrared Heterodyne Spectroscopy of Astronomical and Laboratory Sources at 8.5 μ m. *Nature*, 253, 514-516, Feb. 1975.
8. Frerking, M. A.; and Muehlner, D. J.: Infrared Heterodyne Spectroscopy of Atmospheric Ozone. *Appl. Opt.*, 16, 526-528, 1977.
9. Ku, R. T.; and Spears, D. L.: High Sensitivity Infrared Heterodyne Radiometer Using a Tunable-Diode Laser Local Oscillator, *Optics Lett.*, 1, 84-86, 1977.
10. Harward, C.: The Evaluation of a HgCdTe Photomixer with a Tunable Diode Laser (TDL) and the Evaluation of TDL's as a Local Oscillator in a Heterodyne Detection System. Final Report for NASA Grant NSG 1197, Technical Report PGSTR-AP 77-63, Nov. 1977.
11. Harward, C.; and Hoell, J.: Optical Feedback Effects on the Performance of Pb_{1-x}Sn_xSe Semiconductor Lasers. *Appl. Opt.* 18, 3978, 1979.
12. Allario, F.; Hoell, Jr.; Katzberg, S.; and Larsen, J.: An Experimental Concept to Measure Stratospheric Trace Constituents by Laser Heterodyne Spectroscopy. Accepted for publication in *Applied Physics*, 1980.

13. Savage, M.; Augeri, R.; and Peyton, B. J.: Application of Tunable Diode Lasers to Infrared Heterodyne Spectroscopy. Second Conference on Lasers and Applications, Orlando, FL, Dec. 17-21, 1979.
14. Goldman, A.; and Blatherwick, R. D.: New Atlas of IR Solar Spectra. National Science Foundation, Annual Report for Grant ATM 76-83908, 1978.
15. Brockman, P.; Bair, C.; and Allario, F.: High Resolution Spectral Measurement of the HNO_3 11.3 μm Band Using Tunable Diode Lasers. Appl. Opt., 17, 91, 1978.
16. McClutchey, R.; Benedict, W.; Clough, S.; Burch, D.; Calfee, R.; Fox, K.; Rothman, L.; and Garing, J.: AFCRL Atmospheric Absorption Line Parameter Compilation. Environmental Research Paper 434, AFCRL-TR-73-0096, Jan. 1973.

Table 1. Approximate wave number range and atmospheric species which cause the absorption.

<u>WAVE NUMBER RANGE (cm⁻¹)</u>	<u>ABSORBING SPECIES</u>
1064.0 - 1064.6	O ₃
1066.2 - 1067.1	O ₃ , CO ₂ , H ₂ O
1068.3 - 1069.4	O ₃ , CO ₂
1070.9 - 1071.7	O ₃
1072.8 - 1073.7	CO ₂ , O ₃
1075.0 - 1076.0	O ₃ , H ₂ O
1077.4 - 1078.2	O ₃ , CO ₂
1079.4 - 1080.2	O ₃ , CO ₂
1081.8 - 1082.5	CO ₂ , O ₃
1084.2 - 1085.0	CO ₂ , O ₃
1086.5 - 1087.2	CO ₂ , O
1088.7 - 1089.3	O ₃ , CO ₂
1091.2 - 1091.8	H ₂ O, O ₃
1092.7 - 1093.2	O ₃
896.0 - 896.6	HNO ₃ , CO ₂ , H ₂ O
921.1 - 921.6	H ₂ O, NH ₃

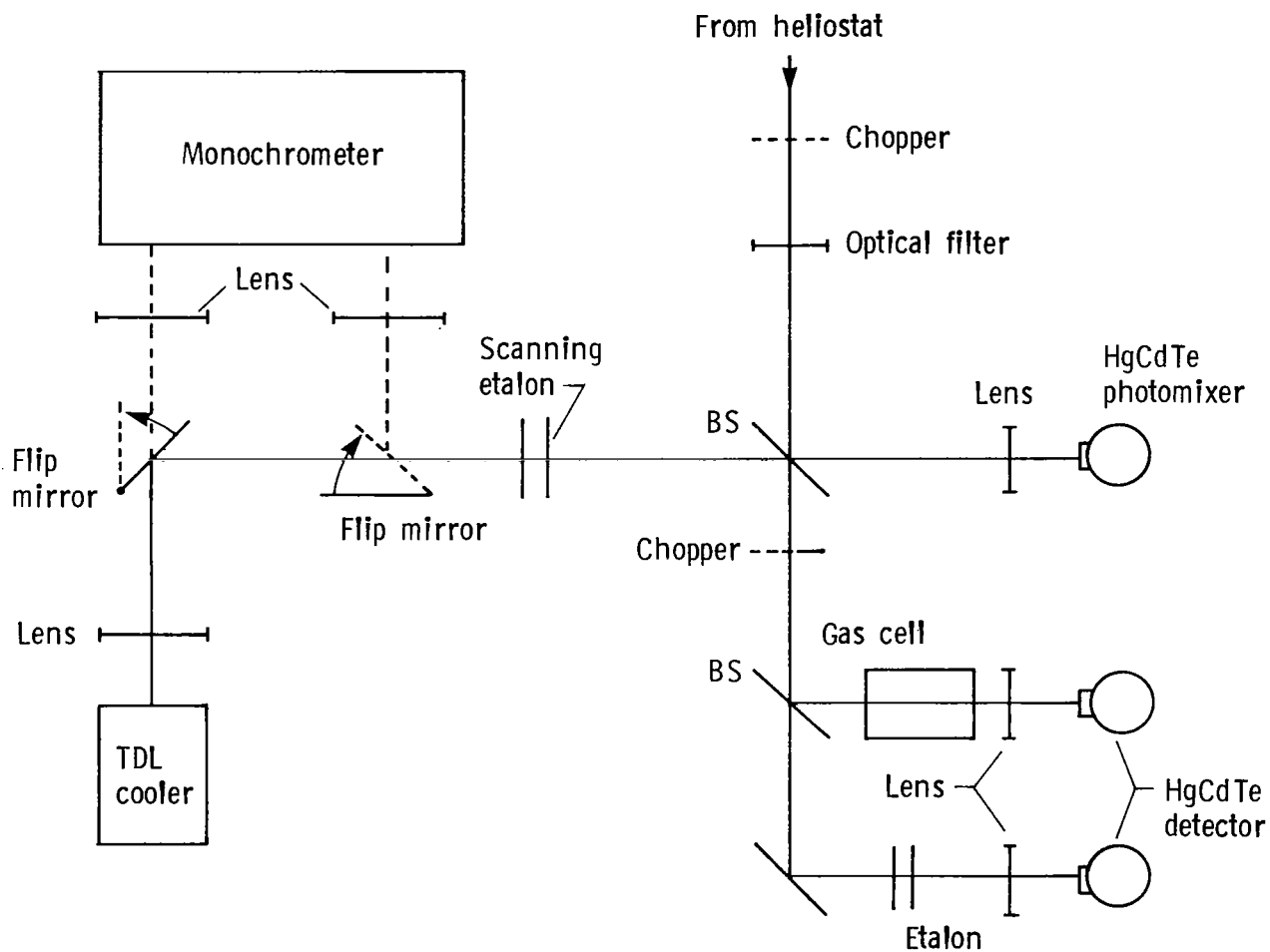
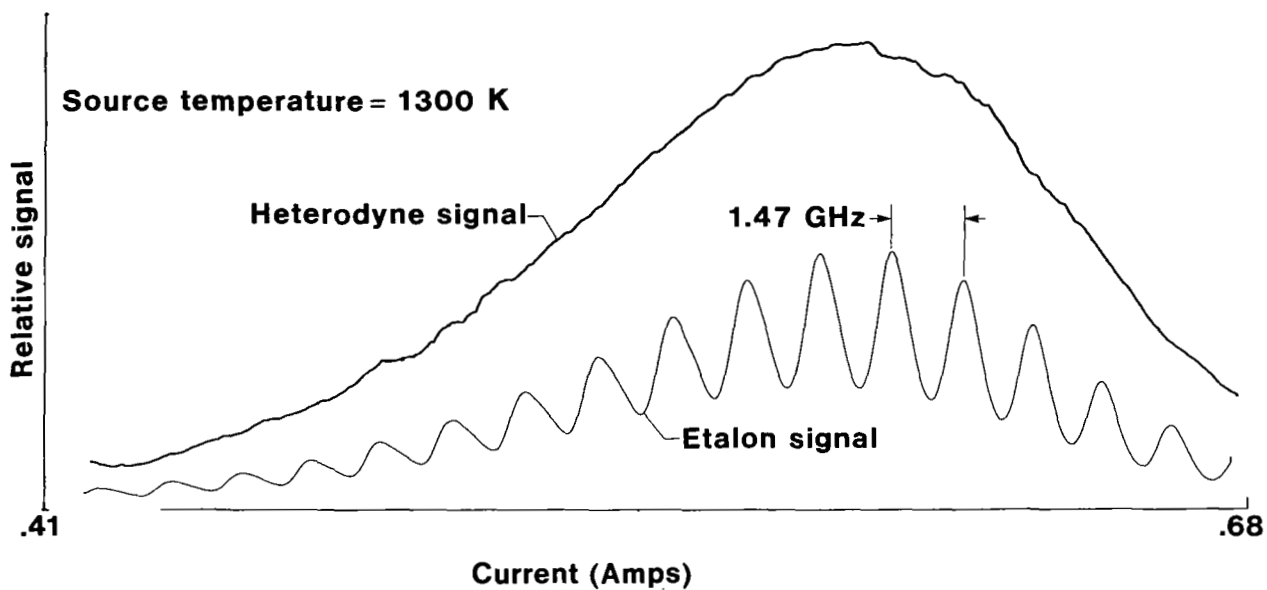
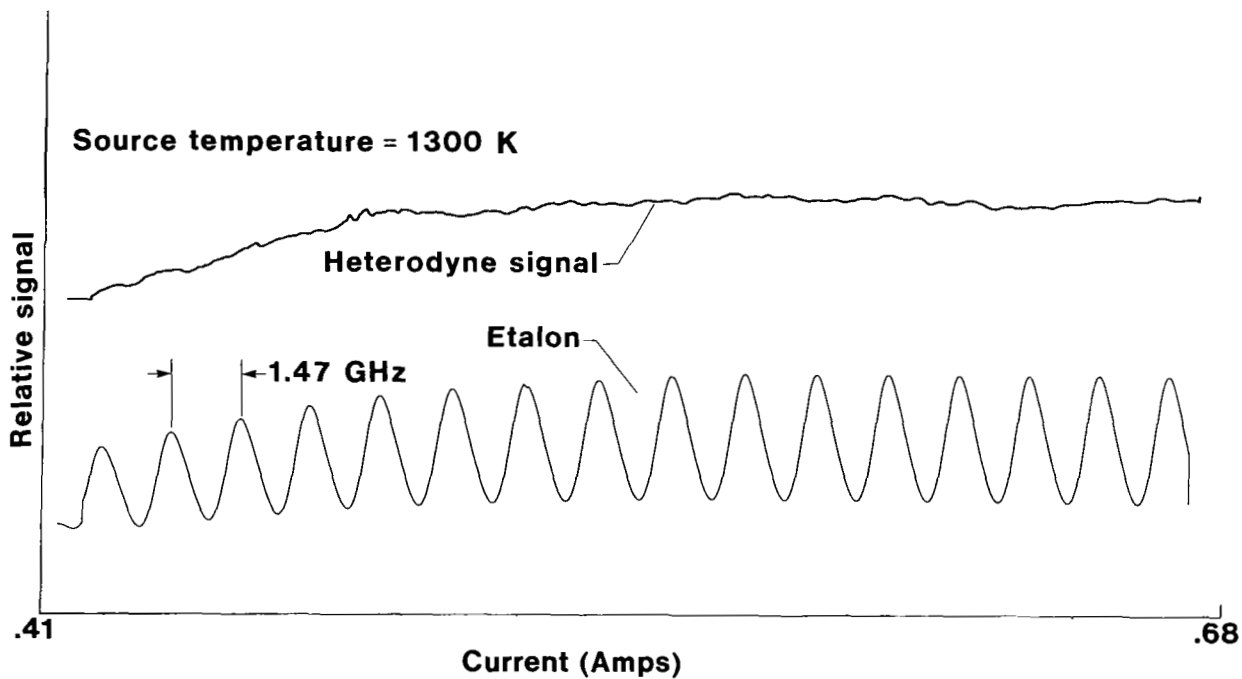


Figure 1.- Optical schematic of the tunable infrared heterodyne radiometer.



(a) Blackbody (1300K) heterodyne signal obtained with a TDL mode isolated with a fixed spacing on the scanning etalon in figure 1.



(b) Same as in (a) above except the scanning etalon was locked to the TDL mode using a conventional feedback circuit.

Figure 2.- Effect of TDL mode isolation technique on blackbody heterodyne signal.

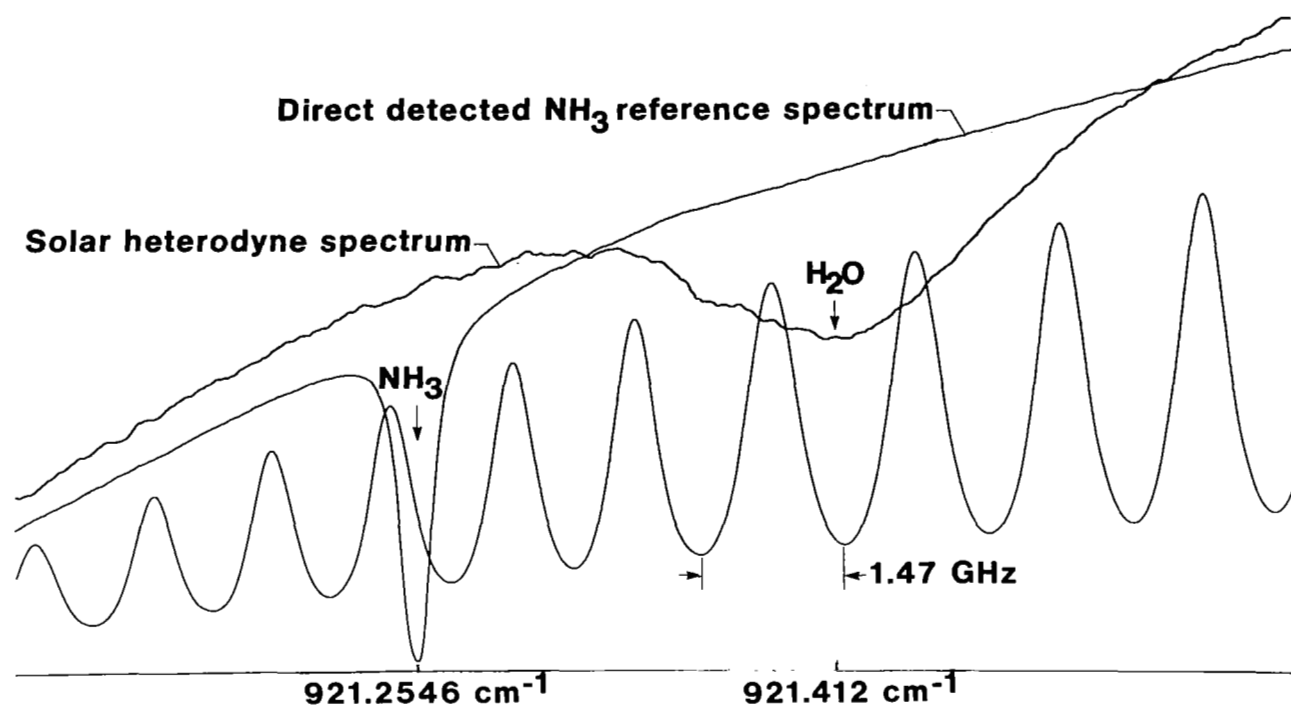


Figure 3.- Heterodyne solar absorption spectrum of atmospheric water vapor with NH_3 as the reference gas.

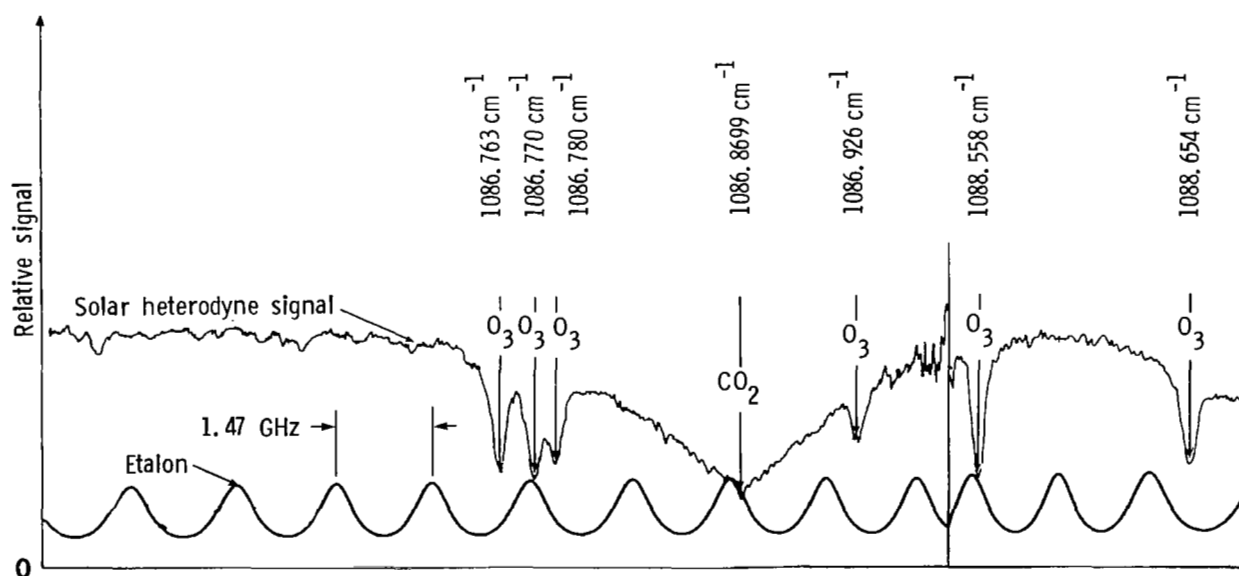


Figure 4.- Heterodyne solar absorption spectra of atmospheric ozone and CO_2 . The absolute wavelength was identified by the broad atmosphere $\text{R}(34) (00^0_1 - 02^0_0) \text{CO}_2$ line.

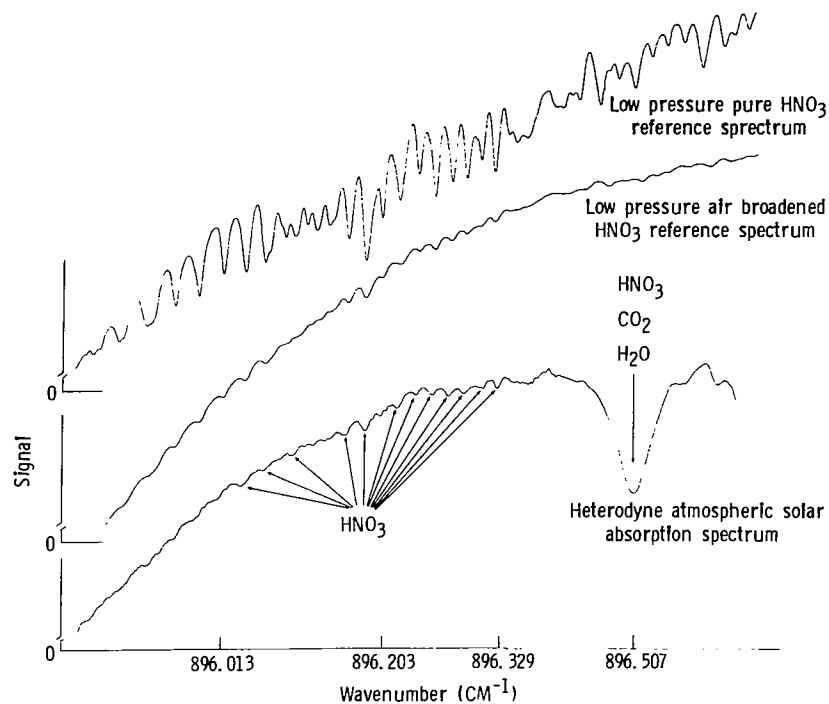


Figure 5.- Heterodyne solar absorption spectrum compared to two HNO_3 reference spectra.

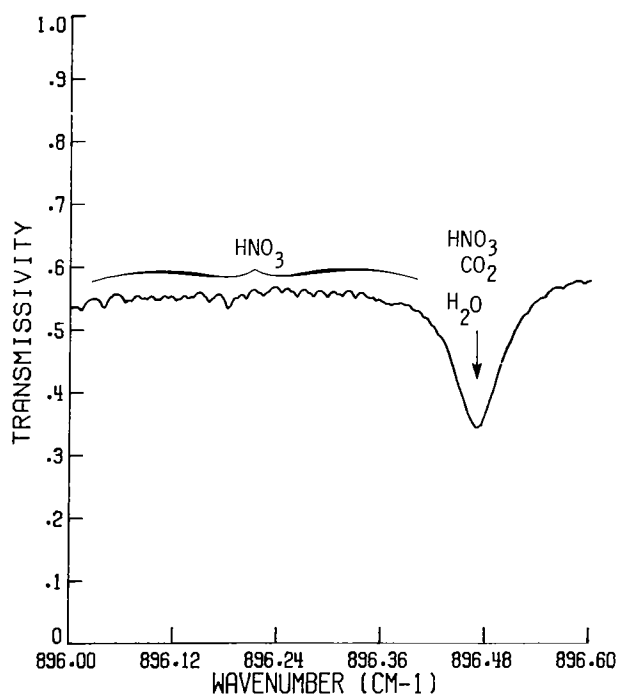


Figure 6.- Synthetic atmospheric spectrum in the same spectral region as shown in figure 5.